Available online at www.sciencedirect.com
SCIENCE DIRECT®
International Journal of Heat and Mass Transfer 48 (2005) 5240–5254
International Journal of HEAT and MASS TRANSFER
www.elsevier.com/locate/ijhmt

Experimental and theoretical analysis of heat and mass transfer in a packed column dehumidifier/regenerator with liquid desiccant

G.A. Longo *, A. Gasparella

Department of Management and Engineering, University of Padova, Stradella S. Nicola 3, I-36100 Vicenza, Italy

Received 15 November 2004
Available online 26 September 2005

Abstract

This paper presents the experimental tests and the theoretical analysis on the chemical dehumidification of air by a liquid desiccant and desiccant regeneration in an absorption/desorption column with random packing.

The experimental set-up is fully described together with measurements, procedures, data reduction and accuracy. The experimental tests include dehumidification and desiccant regeneration runs carried out with the traditional hygroscopic salt solutions H_2O/LiCl and H_2O/LiBr and the new salt solution H_2O/KCOOH in the typical operative ranges of air conditioning applications.

A theoretical model of the packed column and the relative simulation computer code was developed to predict the performance of the system and to analyse the system sensitivity to the main operating parameters. A fair agreement was found between the experimental tests and the simulation computer code.

The experimental tests and the theoretical analysis show that the chemical dehumidification of air by hygroscopic salt solutions ensures consistent reduction in humidity ratio, which is suitable for applications to air conditioning or drying processes. Moreover, desiccant regeneration requires a temperature level around 40–50 °C which can be easily obtained by using solar energy or heat recovered from an industrial process or from a thermal engine.

1. Introduction

The dehumidification of air may be obtained by cooling the air or increasing the air pressure to reduce its capacity to hold moisture, or by removing moisture from the air with a liquid or a solid desiccant.

Cooling the air below its dew point is the most common dehumidification method, particularly for dew point requirements above 5 °C. This approach is energy expensive as it involves both cooling and heating: in fact the air, after the dehumidification process, must normally be re-heated to obtain the required temperature level.

The sorption dehumidification of air by a desiccant is an interesting alternative to the traditional dehumidification process of cooling air below the dew point. The air may be dehumidified by a liquid desiccant, such as hygroscopic salt or glycol solutions in a spray tower or a packed column, or by a solid desiccant, such as silica gel, zeolites, or activated aluminia in a dehumidification

* Corresponding author. Tel.: +39 0444 998726; fax: +39 0444 998888.
E-mail address: tony@gest.unipd.it (G.A. Longo).

0017-9310/$ - see front matter © 2005 Elsevier Ltd. All rights reserved.
doi:10.1016/j.ijheatmasstransfer.2005.07.011

Nomenclature

a	specific interfacial surface, [m^2/m^3]
c	specific heat, [J/(kg K)]
D	molecular diffusivity, [m^2/s]
d_L	Diameter of the liquid droplets in the air flow, [m]
d_s	Equivalent diameter of packing elements, [m]
f	friction factor
F	mass transfer coefficient, [kmol/(m^2s)]
g	gravitational constant, [m/s^2]
G	air mass flux, [kg/s]
G'	air specific mass flow rate, [kg/(m^2s)]
h	specific enthalpy, [J/kg]
k	mass transfer coefficient, [kmol/(m^2s mole fraction)]
L	desiccant mass flow rate, [kg/s]
L'	desiccant mass flux, [kg/(m^2s)]
M	molar mass, [kmol/kg]
N	specific interfacial mole flow rate, [kmol/(m^2s)]
P	pressure, [Pa]
Pr	Prandtl number
q	heat flux, [W/m^2]
r	latent heat, [J/kg]
Re	Reynolds number
Sc	Schmidt number
t	temperature, [K]
U	superficial velocity, [m/s]
X	desiccant concentration, [$kg_{salt}/kg_{solution}$]
X_M	molar concentration of water in the solution, [$kmol_{water}/kmol_{solution}$]
Y	humidity ratio, [$kg_{water}/kg_{dry\ air}$]
Y_M	Molar concentration of water in air, [$kmol_{water}/kmol_{air}$]
Z	co-ordinate along the column, [m]
α	heat transfer coefficient, [W/(m^2K)]
α'	corrected heat transfer coefficient, [W/(m^2K)]
ε	void space in the packing, [$m^3_{voids}/m^3_{packed\ volume}$]
ε_{L0}	operating void space in the packing, [$m^3_{voids}/m^3_{packed\ volume}$]
ε_C	column efficiency
Φ_{Lt}	total liquid hold-up, [$m^3_{liquid}/m^3_{packed\ volume}$]
Φ_{LO}	moving liquid hold-up, [$m^3_{liquid}/m^3_{packed\ volume}$]
Φ_{LS}	static liquid hold-up, [$m^3_{liquid}/m^3_{packed\ volume}$]
λ	thermal conductivity, [W/(m K)]
μ	dynamic viscosity, [kg/(m s)]
ρ	density, [kg/m^3]
σ	surface tension, [N/m]
Δ	difference

Subscripts

C	column
d	dry column
G	air side
i	interfacial
I	inlet
L	desiccant side
max	maximum
min	minimum
O	outlet
t	total
V	water vapour
W	irrigated column
0	reference condition

wheel. The moisture ab/adsorbed in the dehumidification process is removed from the desiccant (regeneration process) by heating. These processes are also useful in reducing airborne microbial and dust contamination.

Desiccant dehumidification systems are successfully competing in applications with large latent loads and/or low dew point requirements (supermarkets, ice rinks, indoor pools, buildings ventilation systems), or where high humidity causes damage to property (storage areas) and where a high indoor air quality is requested (hospitals, laboratories, food and pharmaceutical industries). At present desiccant wheels based on solid sorbent are the most widespread desiccant dehumidification equipment; they are particularly suitable for obtaining an extremely low dew point and require low maintenance. Nevertheless, liquid desiccant units present several design and performance advantages over solid desiccant equipment. They require a lower temperature level for regeneration which is compatible with the use of solar energy or waste heat, whereas the regeneration process in the dehumidification wheels is generally driven by natural gas or electricity. They could be more easily integrated within HVAC plants and have a higher efficiency in removing bacteria and dust from the air [1] than solid sorbent systems. Moreover the cost of a liquid desiccant dehumidifier is lower than a solid desiccant wheel.

The use of a hygroscopic salt solution or a glycol solution has important effects on the characteristics of the liquid desiccant system. Glycols work well as desiccants and are less corrosive than hygroscopic salt solutions. However, glycols have a significant vapour pressure and might evaporate thereby contaminating both process and regeneration air streams, whereas

hygroscopic salts have essentially zero vapour pressure and therefore cannot evaporate into the air streams. Evaporation losses into the air streams increase cost and are unacceptable in air conditioning of an occupied building: therefore hygroscopic salt solutions dominate liquid desiccants commercial applications.

Dehumidification units based on hygroscopic salt solution (H_2O/LiCl) have been commercially available since about 1937, and have been used in a variety of industrial and commercial HVAC systems [2]. More recently, in 1997, a H_2O/LiCl compact air conditioning system, which includes a dehumidification and a regeneration unit integrated with a regenerative heat pump, was commercialised [3].

In open literature several works are available on the theoretical analysis and the computer simulation of heat and mass transfer in the packed columns for chemical dehumidification of air and desiccant regeneration [4–11] together with experimental data on the performance of absorption/desorption packed columns working with hygroscopic salt solutions [11–17]. The theoretical models developed range from complex finite difference models [5,6] to simplified models based on the effectiveness-NTU approach [7,9] or the dimensionless vapour pressure and temperature difference ratios [10]. The experimental works refer mainly to H_2O/LiCl [11,15,16,18] and H_2O/LiBr [5,12,14,17] whereas experimental data are available also for H_2O/LiCl–$CaCl_2$ [13] and H_2O/KCOOH [17] solutions.

This paper presents the experimental tests on the sorption dehumidification of air by a liquid desiccant and desiccant regeneration carried out in an absorption/desorption column with random packing by using the traditional hygroscopic salt solutions H_2O/LiCl and H_2O/LiBr and the new salt solution H_2O/KCOOH in typical operative ranges of air conditioning applications. This paper also presents a theoretical analysis and the relative simulation computer code of the heat and mass transfer processes inside a packed column dehumidifier/regenerator with liquid desiccants.

2. Experimental set-up, procedures and data reduction

The experimental rig, shown in Fig. 1, consists of an air loop and a desiccant loop. In the first loop ambient air is heated and humidified to achieve the set conditions at the inlet of the packed column. The power of the heating element can be varied from 0 to 2000 W by a PID controller, while the steam humidifier provides a vapour flow rate from 0 to 5 kg/h. The air goes through the packed column, where the heat and mass transfer with the desiccant takes place in a counter-flow configuration (air up-flow and desiccant down-flow), and then it is discharged. An air dehumidification process or a desiccant regeneration process occurs depending on the relative values of the partial vapour pressure on the air and solution side. The column shell, made of stainless steel, 725 mm in height and 400 mm in diameter, is filled with randomly packed 25 mm plastic Pall Rings supported by a stainless steel net and sprinkled with a 12 hole liquid distributor. A large chamber at the bottom of the column provides a good air distribution, whereas a stainless steel wire mesh at the top removes desiccant droplets carried by the air at the highest velocities. The air duct, manufactured from a 160 mm diameter PVC tube, contains two measurement sections located at the inlet and at the outlet of the column to measure temperature and humidity ratio.

Each measuring station consists of two temperature taps, instrumented with T-type thermocouples (accuracy within ±0.1 K), and two humidity taps, connected to dew point temperature probes (accuracy within ±0.2 K), placed at different positions in the gas flow. The pressure drop of the air flow through the column is measured by a strain-gage differential pressure transducer (accuracy

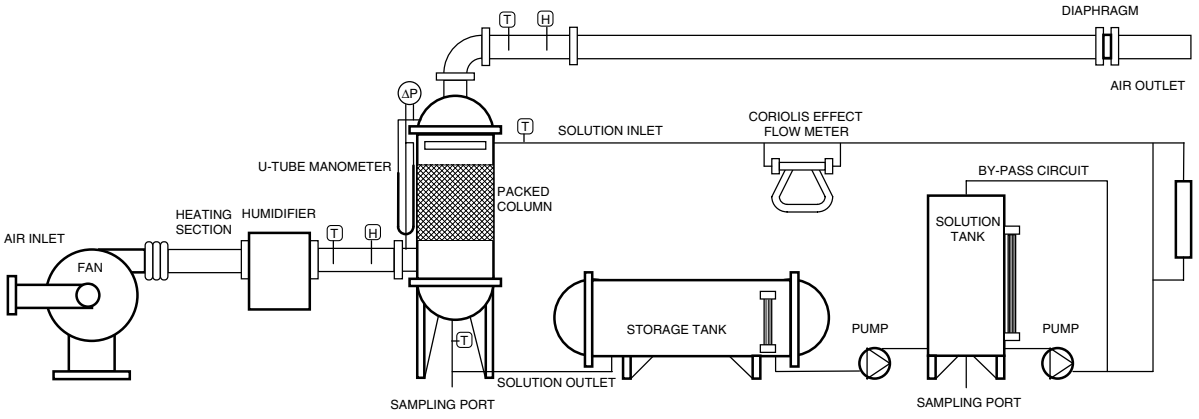

Fig. 1. Schematic view of experimental test rig.

within ±0.1% f.s.) and also by a U-tube manometer, while the air flow rate is measured by a diaphragm (accuracy within ±2.0%) inserted in the air duct at the outlet of the column after 3000 mm of straight tube. The absolute atmospheric pressure is measured by a barometer (accuracy of ±0.08% f.s.).

The desiccant is maintained at a constant temperature and at a uniform concentration in a stainless steel tank by a PID controller. From there it is pumped into the dehumidifier/regenerator and sprinkled onto the packed column. The solution, after the heat and mass transfer with air, flows due to gravity into a storage tank. The flow rate of the desiccant, varied by the by-pass valve of the solution tank, is measured by a Coriolis effect mass flow meter (accuracy within ±0.1% of the measured value) and also by evaluating the variation of the liquid level in the tank at any fixed time. The temperature of the solution is measured at the inlet and outlet of the column by T-type thermocouples (accuracy within ±0.1 K), whereas the concentration at the inlet and outlet is derived from density measurements on samples carried out with a density meter (accuracy within ±0.1 kg/m^3 for density and within ±0.01 K for temperature measurement).

The readings of the thermocouples, the hygrometers, the Coriolis effect mass flow meter and the differential pressure transducer are scanned and recorded by a data logger, whereas the measurements of the air flow rate and the solution concentration are taken manually and then implemented into the computer.

Table 1 gives the main features of the different measuring devices in the experimental rig.

In the present work both air dehumidification and solution regeneration tests were carried out. Before starting each test the solution in the tank was recirculated through the by-pass circuit to ensure uniform conditions. The air and desiccant flow rates were then established at set values, while temperature, humidity and mass flow rate readings were recorded. Once temperature and humidity steady state conditions were achieved, readings were collected. Manual flow and pressure drop measurements were repeated three times, samples of the solution were taken at the inlet and outlet of the column to measure its concentration. From the measurements collected, a computer code calculated the heat and mass balances over the column to determine the moisture content change and the temperature variation for both the air and the solution flows. The experimental results are reported in terms of air humidity reduction, desiccant concentration variation and pressure drop on the air side through the packed column.

The performance of a dehumidification/regeneration column can be evaluated by a specific column efficiency which is defined as the ratio between the absolute value of the actual humidity change on the air side and the absolute value of the maximum humidity change possible under given conditions:

$$\varepsilon_C = |Y_I - Y_O|/|Y_I - Y_{O\cdot min/max}| \quad (1)$$

where Y is the air humidity ratio, while I and O subscripts refer to inlet and outlet sections of the column. The maximum humidity change is achieved when the partial vapour pressure of the air at the outlet is equal to the saturation pressure of the solution at the inlet of the column. This efficiency is valid both for dehumidification and regeneration tests.

3. Theoretical analysis and simulation computer code

3.1. Heat and mass transfer analysis

The theoretical analysis of the heat and mass transfer in a packed column was derived from Treybal's work [4] on adiabatic gas absorption in accordance with [5,6].

The model is based on the following assumptions:

- the system is adiabatic,
- the thermal resistance in the liquid phase is negligible compared to the gas phase,
- the heat and mass transfers occur only in transversal direction to gas and liquid flows,
- the interface areas active in heat and mass transfer processes are the same.

Fig. 2 shows a differential control volume of the column 1 m^2 in cross section area and dZ in height: the heat

Table 1
Specification of the different measuring devices

Devices	Type	Accuracy	Range
Thermometers	Thermocouple T	0.1 K	0–60 °C
Dew point probes	Mirror probe	0.2 K	−50/+50 °C
Solution flow meter	Coriolis effect flow meter	0.1%	0–1600 kg/h
Density meter	Oscillator cell	0.1 kg/m^3 and 0.01 K	1–9999 kg/m^3
Differential pressure transducer	Strain gage	0.1% f.s.	0–10 mbar
Barometer	Strain gage	0.08% f.s.	800–1200 mbar
Air flow meter	Diaphragm	2%	0–800 m^3/h

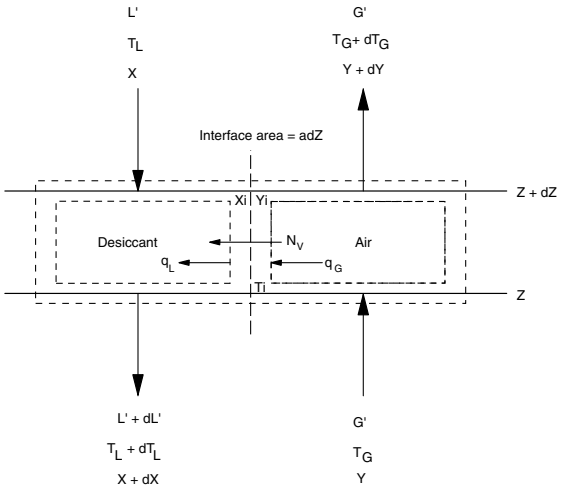

Fig. 2. Differential section of a packed column.

and mass transfer takes place at the interface between solution and air in a counter-flow configuration.

The enthalpy of the desiccant with respect to a reference temperature t_0 results:

$$h_L = c_L(t - t_0) + \Delta h_S \tag{2}$$

where c_L is the specific heat and Δh_S the dilution heat of the solution at the reference temperature. The specific enthalpy of air is:

$$h_G = c_G(t - t_0) + Y[c_V(t_G - t_0) + r_0] \tag{3}$$

with Y humidity ratio, c_G and c_V specific heat for dry air and steam respectively, r_0 water latent heat at the reference temperature.

The mass conservation equation for the water content gives:

$$dL' = G'dY \tag{4}$$

where L' and G' are the mass flux for the liquid and the gas phase.

The mass transfer at the interface results:

$$N_V M_V a\,dZ = -G'dY \tag{5}$$

where "a" is the specific interfacial surface (m^2 of interface/m^3 of packed volume) and is a function of the packing structure, M_V is the water molar mass and N_V the specific interfacial mole flow rate. The latter parameter can be related to the interfacial Y_{Mi} and bulk Y_M molar concentration of water in the air flow by the following correlation:

$$N_V = F_G \ln[(1 - Y_{Mi})/(1 - Y_M)] \tag{6}$$

where F_G is the air mass transfer coefficient. The molar concentration Y_M is correlated to the humidity ratio by the relation:

$$Y_M = p_{VG}/p_t = Y/(Y + M_V/M_G) \tag{7}$$

where p_{VG} and p_t are vapour partial pressure and total pressure in humid air respectively and M_G is the molar mass of dry air. If the interfacial mass transfer resistance in the liquid phase is negligible, the interfacial vapour pressure is equal to that in the solution and Eq. (6) becomes:

$$N_V = F_G \ln[(1 - p_{VL}/p_t)/(1 - p_{VG}/p_t)] \tag{8}$$

The air mass transfer coefficient F_G can be computed by the following empirical correlation [4]:

$$F_G = 1.195G\{d_s G'/[\mu_G(1 - \varepsilon_{L0})]\}^{-0.36} Sc_G^{-0.667} \tag{9}$$

where d_s is the equivalent diameter of the packing elements available in [4], μ_G is the air dynamic viscosity, ε_{L0} is the operating void space in the packing and Sc_G the Schmidt number for the air.

The operating void space in the packing ε_{L0} is equal to the void space of the dry packing minus the total liquid hold-up Φ_{Lt}:

$$\varepsilon_{L0} = \varepsilon - \Phi_{Lt} \tag{10}$$

The total liquid hold-up consists of the "moving hold-up" Φ_{LO} (liquid retained in the packing and continually replaced by fresh liquid) and the "static hold-up" Φ_{LS} (liquid retained in the interstices of the packing and only slowly replaced by fresh liquid):

$$\Phi_{Lt} = \Phi_{LO} + \Phi_{LS} \tag{11}$$

In [4] it is possible to find the hold-up correlations for different packing elements.

The Schmidt number results:

$$Sc_G = \mu_G/\rho_G D_G \tag{12}$$

where ρ_G and D_G are the density and the molecular diffusivity of air.

The interfacial area for absorption process with water or aqueous solutions can be evaluated by the following equation [4]:

$$a = m(808G'/\rho_G^{0.5})^n L'^p \tag{13}$$

The coefficients m, n and p for different packing elements are available in [4]. From Eqs. (5) and (6) it is possible to obtain:

$$-G'\,dY = (M_V F_G a\,dZ)\ln[(1 - Y_{Mi})/(1 - Y_M)] \tag{14}$$

and so the basic differential equation for the air humidity ratio results:

$$(dY/dZ) = -(M_V F_G a/G')\ln[(1 - Y_{Mi})/(1 - Y_M)] \tag{15}$$

The interfacial molar concentration Y_{Mi} in the gas phase can be calculated by considering the mass balance at interface. The specific interfacial mass transfer on solution side results:

$$N_L = F_L \ln[(1 - X_M)/(1 - X_{Mi})] \tag{16}$$

where X_M and X_{Mi} are the bulk and interfacial solution's molar concentration in water, while F_L is the mass transfer coefficient in the desiccant equal to:

$$F_L = k_L(\rho_L/M_L)X_{MBM} \tag{17}$$

where X_{MBM} is the average solution's molar concentration in salt, while M_L is the average molar mass of the solution. The liquid-phase mass transfer coefficient k_L can be calculated by the following empirical correlation [4]:

$$k_L = 25.1(D_L/d_s)(d_sL'/\mu_L)^{0.45}Sc_L^{0.5} \tag{18}$$

where μ_L is the desiccant dynamic viscosity and Sc_L the Schmidt number for the desiccant equal to:

$$Sc_L = \mu_L/\rho_L D_L \tag{19}$$

where D_L is the molecular diffusivity of desiccant.

By equating the specific interfacial mass transfer on the air side (Eq. (6)) to that on the desiccant side (Eq. (16)) it is possible to derive the following expression for the interfacial molar concentration in water on the air side:

$$Y_{Mi} = 1 - (1 - Y_M)[(1 - X_M)/(1 - X_{Mi})]^{F_L/F_G} \tag{20}$$

This equation has to be solved simultaneously with the vapour–liquid equilibrium equation for the solution by an iterative procedure.

The simultaneous heat transfer results:

$$q_G a\,dZ = \alpha'_G a(t_G - t_i)\,dZ \tag{21}$$

where q_G is the sensible heat flux on the air side; α'_G is the air heat transfer coefficient corrected to account for simultaneous mass transfer (Ackermann correction), t_G and t_i are the bulk and interfacial air temperature. The Ackermann correction for simultaneous mass transfer gives:

$$\alpha'_G a = N_V M_V c_V a/[1 - \exp(-N_V M_V c_V a/\alpha_G a)] \tag{22}$$

where α_G is the heat transfer coefficient for the air. Considering Eqs. (5), Eq. (22) becomes:

$$\alpha'_G a = -G' c_V(dY/dZ)/[1 - \exp(G' c_V(dY/dZ)/\alpha_G a] \tag{23}$$

The heat transfer coefficient for air α_G can be calculated by the following equation:

$$\alpha_G = 1.195G' c_G\{d_sG'/[\mu_G(1 - \varepsilon_{L0})]\}^{-0.36}Pr_G^{-0.667} \tag{24}$$

derived from Eq. (9) by the analogy between heat and mass transfer. The Schmidt number in Eq. (9) has been replaced by the air Prandlt number:

$$Pr_G = \mu_G c_G/\lambda_G. \tag{25}$$

The thermal balance on the air side results:

$$G'h_G - G'(h_G + dh_G) + G'\,dY\,[c_V(t_G - t_0) + r_0] = \alpha'_G a(t_G - t_i)\,dZ \tag{26}$$

where the air enthalpy variation across the differential element results:

$$dh_G = c_G\,dt_G + Yc_V\,dt_G + dY[c_V(t_G - t_0) + r_0] \tag{27}$$

Rearranging Eqs. (26) and (27) it is possible to obtain the basic differential equation for the air temperature:

$$(dt_G/dZ) = -\alpha'_G a(t_G - t_i)/[G'(c_G + Yc_V)] \tag{28}$$

The overall thermal balance on the differential control volume of the column gives:

$$L'\,dh_L + G'\,dYh_L = G'\,dh_G \tag{29}$$

Considering Eqs. (2) and (27), Eq. (29) becomes:

$$L'[c_L\,dt_L + d(\Delta h_S)] + G'\,dY[c_L(t_L - t_0) + \Delta h_S] = \{c_G\,dt_G + Yc_V\,dt_G + dY[c_V(t_G - t_0) + r_0]\}G' \tag{30}$$

Neglecting the variation of dilution heat $d(\Delta h_S)$ from Eq. (30) it is possible to obtain the basic differential equation for the desiccant temperature:

$$(dt_L/dZ) = (G'/L'c_L)\{(c_G + Yc_V)(dt_G/dZ) + [c_V(t_G - t_0) + r_0](dY/dZ) - [c_L(t_L - t_0) + \Delta h_S](dY/dZ)\} \tag{31}$$

The mass conservation equation for the salt content on the differential control volume gives:

$$L'X = (L' + dL')(X + dX) \tag{32}$$

where X is the desiccant concentration in salt.

Rearranging Eq. (32) and considering Eq. (4) it is possible to obtain the basic differential equation for the desiccant concentration in salt:

$$(dX/dZ) = -[X\,dL'/L']/dZ = -X(L'/G')\,dY/dZ \tag{33}$$

3.2. Pressure drop analysis

The analysis of the pressure drop on the air side in a packed column was based on the computation of the dry column pressure drop and a correction term to account for the effect of desiccant flow rate as suggested by Engel et al. [18].

The dry column pressure drop per unit height is given by the following correlation:

$$\Delta P_d = 0.125f(\rho_G U_G^2 a)/\varepsilon^{4.65} \tag{34}$$

where U_G is the air superficial velocity and f is the friction factor given by the following equation:

$$f = C_1/Re_G + C_2/Re_G^{0.5} + C_3 \tag{35}$$

as function of the air Reynolds number

$$Re_G = (\rho_G U_G d_s)/\mu_G \tag{36}$$

C_1, C_2 and C_3 constants for different packing elements are available in [19].

The irrigated column pressure drop per unit height will be:

$$\Delta P_w = \Delta P_d[(6\Phi_{LO}/d_L + a)/a][\varepsilon/(\varepsilon - \Phi_{LO})]^{4.65} \quad (37)$$

where d_L is the diameter of the liquid droplets in the air flow and Φ_{LO} is the moving liquid hold-up.

The diameter of the liquid droplets can be computed by equating surface tension and buoyancy force as follows:

$$d_L = C[6\sigma_L/g(\rho_L - \rho_G)]^{0.5} \quad (38)$$

where σ_L is the desiccant surface tension, g the gravitational constant and C a constant equal to 0.4 for random packing.

The moving liquid hold-up Φ_{LO} can be correlated to the irrigated column pressure drop ΔP_w by the following equation:

$$\Phi_{LO} = 3.6[(U_L a^{0.5})/g^{0.5}]^{0.66}[(\mu_L a^{1.5})/(\rho_L g^{0.5})]^{0.25} \times [(\sigma_L a^2)/(\rho_L g)]^{0.1}\{1 + [6\Delta P_w/(\rho_L g)]^2\} \quad (39)$$

The solution of the above nonlinear system of equations (Eqs. (34)–(39)) with two unknown parameters (moving liquid hold-up Φ_{LO} and irrigated column pressure drop ΔP_w) is obtained by an iterative approach.

3.3. Simulation computer code

The basic differential equation for all the characteristic parameters (air and desiccant temperature, air humidity ratio and desiccant concentration) permits simulation of the packed column section by section: a specific simulation computer code was developed.

The whole absorption/desorption column was subdivided into an appropriate number (ten) of sections and suitable subroutines were realised to simulate heat and mass transfer processes between air and desiccant in accordance with the above theoretical analysis and to compute fluids properties. Thermodynamic, thermophysical and transport properties of the desiccant H_2O/LiCl were calculated in accordance with [20–22], whereas the properties of the desiccant H_2O/LiBr were calculated in accordance with [23–26] and the properties of desiccant H_2O/KCOOH were computed in accordance with [27].

Input values were set for inlet conditions (air temperature, humidity ratio and mass flow rate, desiccant temperature, concentration and mass flow rate) and the characteristic parameters of the packed column (packing elements, column transversal cross-area and height). The step-by-step analysis of the packed column was carried out from the base to the top of the column. The outlet desiccant conditions (column base) were initially guessed and iterations were carried out until convergence between calculated and real inlet desiccant conditions (column top) was obtained. The final output

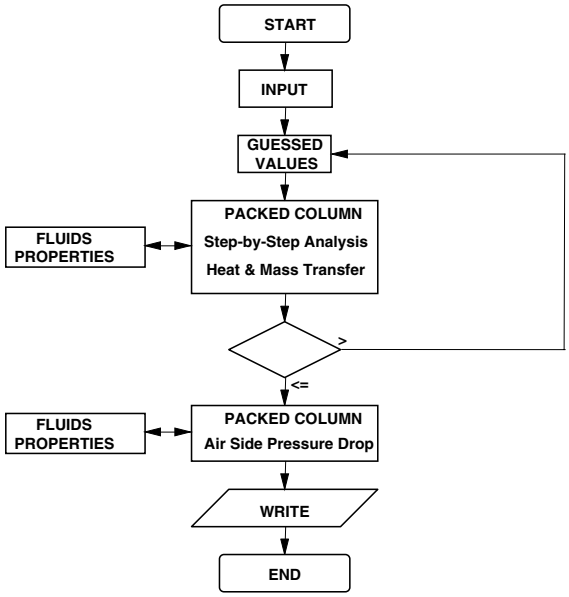

Fig. 3. Flow chart of simulation computer code.

results included the outlet conditions both for air and desiccant together with the temperature, humidity ratio and concentration profiles through the packed column. The simulation computer code also includes a specific subroutine for the computation of the air side pressure drop in the packed column by Eqs. (34)–(39). Fig. 3 shows the flow chart of the whole simulation computer code.

4. Analysis of the results

4.1. Experimental results

Two different sets of experimental tests were carried out: the first included 28 dehumidification runs with H_2O/LiCl, 20 with H_2O/LiBr and 26 with H_2O/KCOOH; the second included 19 regeneration runs with H_2O/LiCl, 26 with H_2O/LiBr and 12 with H_2O/KCOOH. When the partial vapour pressure on the air side was higher than that on the desiccant side a dehumidification process occurred, whereas with a contrary partial vapour pressure gradient a desiccant regeneration process was obtained. Table 2 gives the main operating conditions under experimental tests: air inlet temperature T_{Gi} and humidity ratio Y_i, solution inlet temperature T_{Li} and concentration X_i, air mass flux G' and solution mass flux L', ratio between solution L and air G mass flow rates. The air mass fluxes investigated during experimental tests, lower than the values usually applied in commercial units, were set to ensure zero-carryover conditions and to have a pressure drop

Table 2
Operative conditions under experimental tests

Test	Desiccant	Runs	T_{GI} (°C)	Y_I (g/kg)	T_{LI} (°C)	X_I (%salt)	G' (kg/m^{2}s)	L' (kg/m^{2}s)	L/G
Dehumidification	H_2O/LiCl	28	24.3–37.6	7.3–23.3	23.4–24.0	39.2–40.6	0.43–0.47	0.10–1.17	0.23–2.6
Dehumidification	H_2O/LiBr	20	23.6–36.7	8.2–22.8	23.7	53.9–51.9	0.44–0.47	0.16–1.39	0.35–3.0
Dehumidification	H_2O/KCOOH	26	22.6–35.8	8.8–20.7	21.9–24.8	72.8–74.0	0.48–0.52	0.09–1.23	0.20–2.5
Regeneration	H_2O/LiCl	19	48.2–50.1	4.0–12.3	49.9–50.5	39.1–39.3	0.38–0.42	0.14–1.23	0.35–3.2
Regeneration	H_2O/LiBr	26	50.0	3.0–15.4	48.0–49.5	51.3–50.1	0.40–0.44	0.16–1.46	0.45–3.5
Regeneration	H_2O/KCOOH	12	50.0	2.8–14.5	46.9–50.6	75.5–75.9	0.41–0.44	0.13–1.32	0.31–3.0

similar to conventional dehumidification cooling coils or dehumidification wheels.

During dehumidification tests the solution inlet temperature was around 23–24 °C, whereas regeneration conditions were obtained by increasing the solution and the air inlet temperature up to values around 50 °C.

The concentrations of the different desiccants were set to have similar crystallisation temperatures, from −15 °C to −20 °C, and therefore similar operating ranges.

A detailed error analysis, performed in accordance with [28], indicated an overall accuracy within ±12.7% of humidity reduction, within ±25.9% of desiccant concentration variation and within ±4.9% of pressure drop measurements: Table 3 shows the maximum uncertainty of each set of experimental data.

Fig. 4a–c shows the humidity reduction measured during the dehumidification tests against the ratio between the desiccant mass flow rate L and the air mass flow rate G. The dehumidification rate depends on the mass flow rate ratio with a logarithmic trend, the slope of which increases, in absolute value, with the air inlet humidity ratio. The traditional solutions H_2O/LiCl and H_2O/LiBr show similar dehumidification performances which are higher than the H_2O/KCOOH solution. For example, under an inlet air humidity ratio around 11–12 g/kg and a mass flow rate ratio around 2, H_2O/LiCl and H_2O/LiBr solutions show a dehumidification rate around 6–7 g/kg, whereas the dehumidification rate for H_2O/KCOOH solution is around 5 g/kg. The measured humidity reductions are interesting for applications to air conditioning or drying processes.

Fig. 5a–c show the solution concentration increase measured during the regeneration runs vs. the mass flow rate ratio L/G. The regeneration rate depends on the flow rate ratio with a logarithmic trend, the slope of which decreases with the air inlet humidity ratio. The solution H_2O/KCOOH shows a better regeneration performance than H_2O/LiCl and H_2O/LiBr solutions. For example, under an inlet air humidity ratio around 10–11 g/kg and a mass flow rate ratio around 1, H_2O/LiCl and H_2O/LiBr solutions show a regeneration rate around 0.25%, whereas the regeneration rate for H_2O/KCOOH solution is around 0.45%.

Fig. 6 shows the column efficiency for the experimental tests carried out. The efficiency increases with the mass flow rate ratio, with a similar trend both for dehumidification and regeneration tests but with a different absolute value. Dehumidification efficiency varies between 30% and 90% with a flow rate ratio ranging from 0.2 to 3.0, whereas regeneration efficiency varies from 20% to 75% with a flow rate ratio ranging from 0.3 to 3.5. The efficiency shows negligible sensitivity to desiccant types.

Fig. 7 shows the air side pressure drop per unit height vs. the mass flow rate ratio L/G both for dehumidification and regeneration runs. The experimental pressure drop shows a weak sensitivity to the mass flow rate ratio and desiccant types. The difference in pressure drop between dehumidification and regeneration tests relies on to the different operative conditions on the air side as shown on Table 2.

The experimental results are also compared to the simulation code results for the packed column: Fig. 8 shows the comparison between experimental and

Table 3
Maximum uncertainty of each set of experimental data

Test	Desiccant	Runs	Maximum uncertainty (dehumidification rate)	Maximum uncertainty (regeneration rate)	Maximum uncertainty (pressure drop)
Dehumidification	H_2O/LiCl	28	±8.8%	=	±4.5%
Dehumidification	H_2O/LiBr	20	±5.2%	=	±4.5%
Dehumidification	H_2O/KCOOH	26	±12.7%	=	±4.3%
Regeneration	H_2O/LiCl	19	=	±25.9%	±4.9%
Regeneration	H_2O/LiBr	26	=	±14.8%	±4.9%
Regeneration	H_2O/KCOOH	12	=	±13.5%	±4.8%

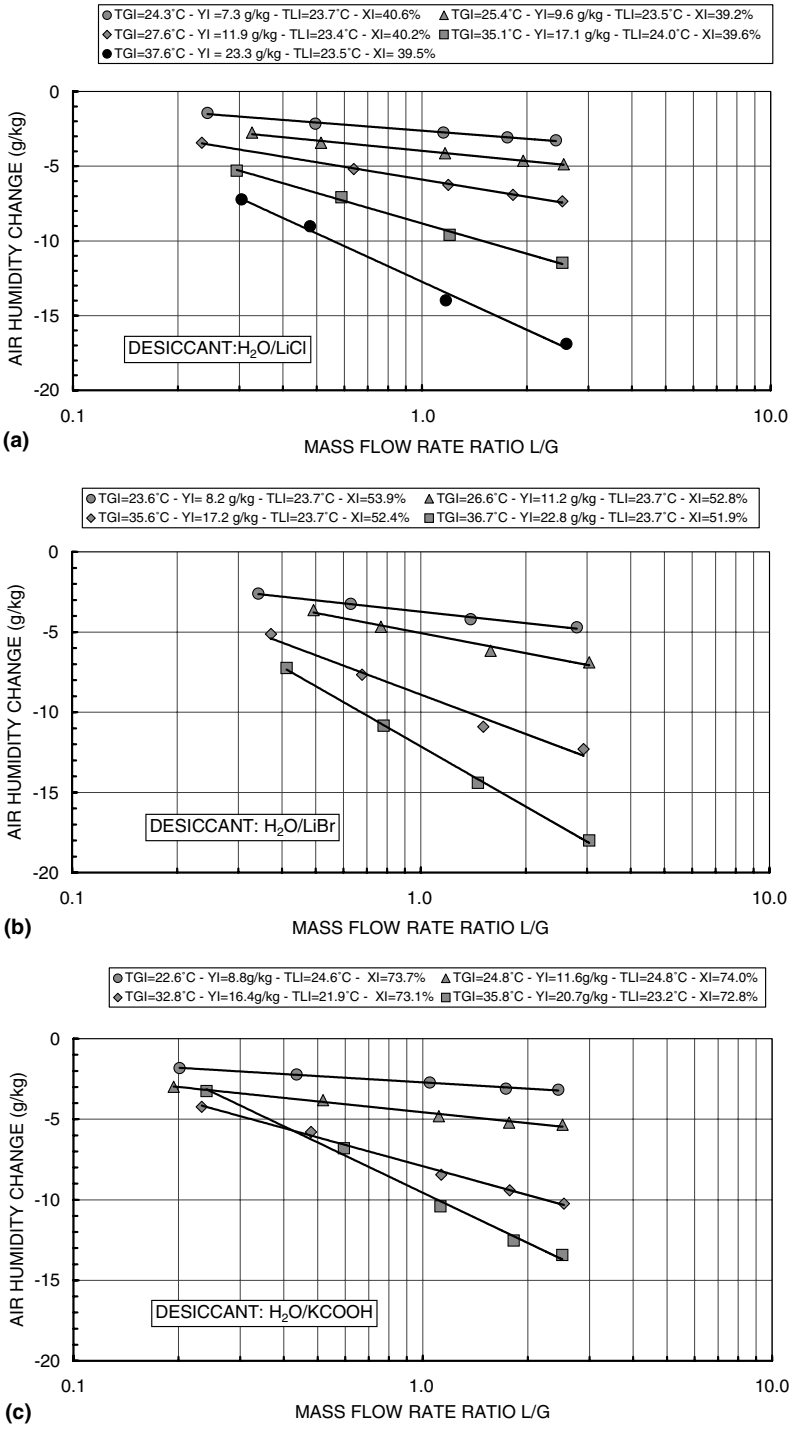

Fig. 4. Humidity reduction vs. mass flow rate ratio L/G under dehumidification experimental tests with desiccant: (a) H_2O/LiCl, (b) H_2O/LiBr and (c) H_2O/KCOOH.

calculated air humidity reduction during dehumidification tests, Fig. 9 shows experimental versus calculated solution concentration increase during regeneration tests, whereas Fig. 10 shows the comparison between experimental and calculated pressure drop. The simulation code reproduces dehumidification runs with a mean

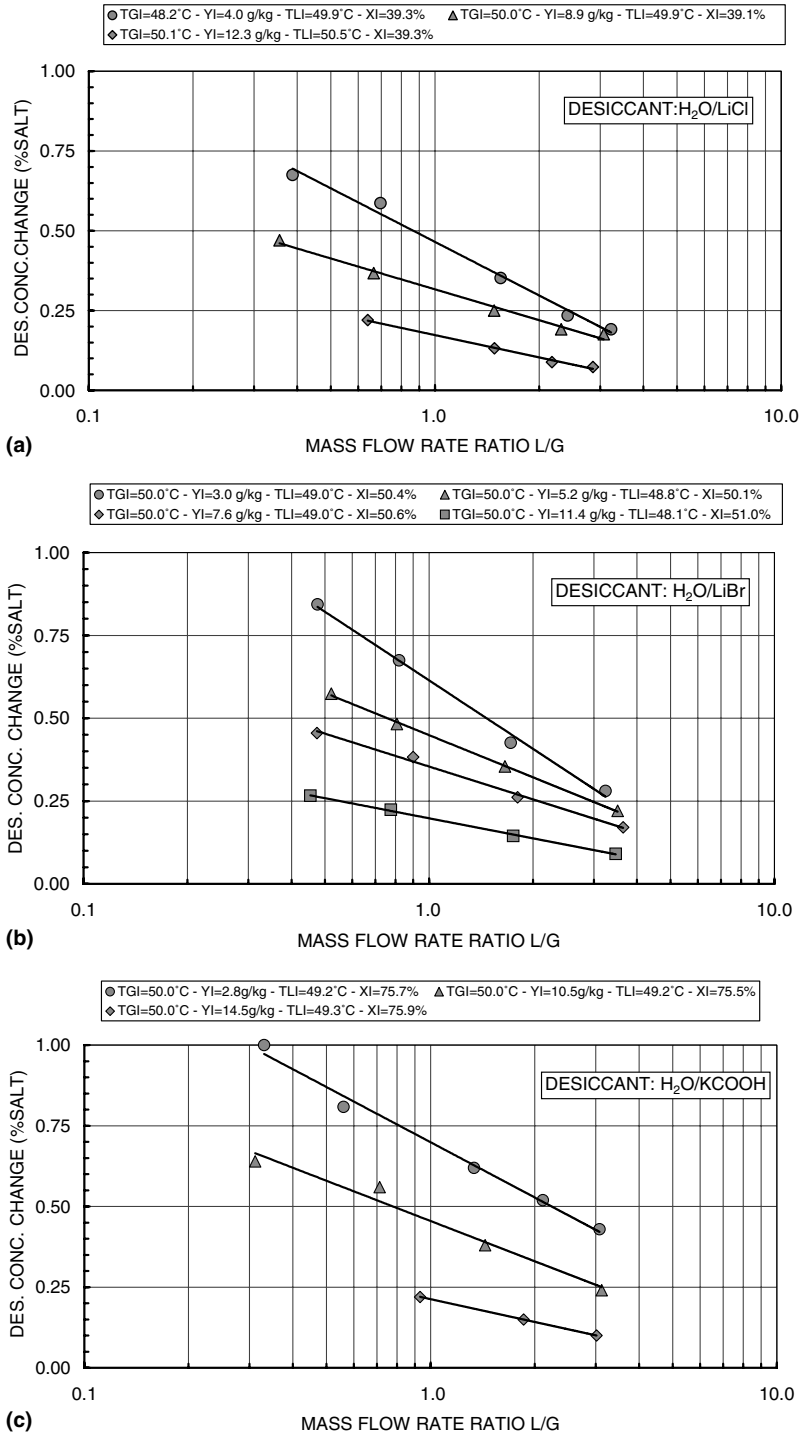

Fig. 5. Desiccant concentration increase vs. mass flow rate ratio L/G under regeneration experimental tests with desiccant: (a) H_2O/LiCl, (b) H_2O/LiBr and (c) H_2O/KCOOH.

absolute deviation of 8.8%, regeneration tests with a mean absolute deviation of 14.8% and pressure drop measurements with a mean absolute deviation of 9.4%: Table 4 shows the mean absolute deviation of the model

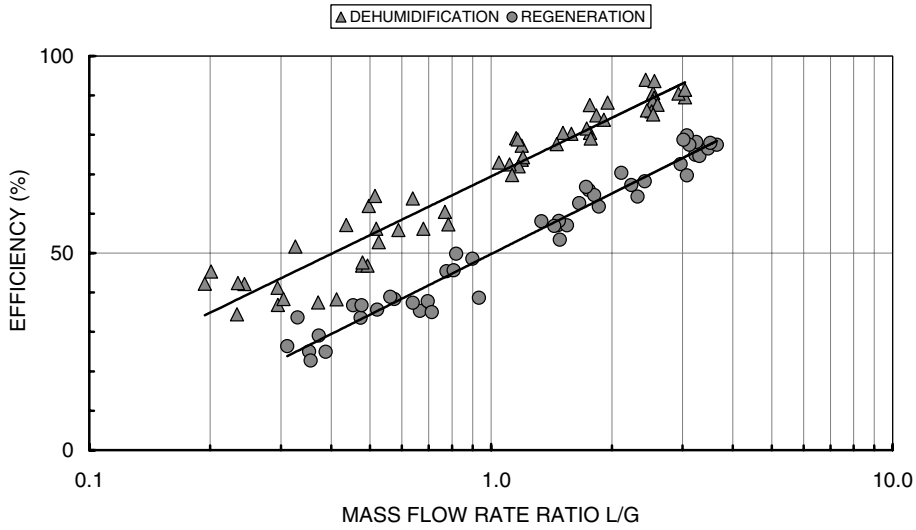

Fig. 6. Packed column efficiency vs. mass flow rate ratio under dehumidification and regeneration experimental tests.

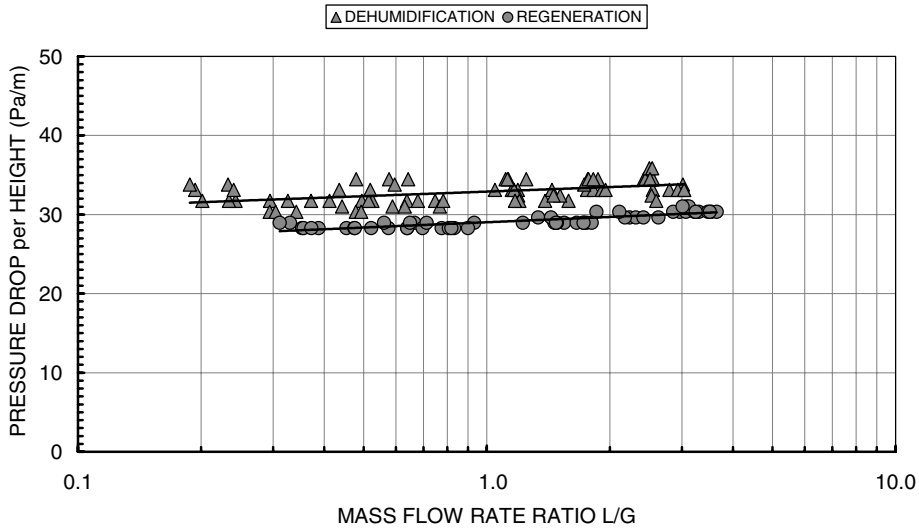

Fig. 7. Air side pressure drop per unit height vs. mass flow rate ratio under dehumidification and regeneration experimental tests.

for each set of data. Therefore the model reproduces the dehumidification and regeneration rates within their experimental accuracy and it appears fully adequate to simulate the investigated processes.

4.2. Simulation results

A parametric study was carried out to evaluate the system sensitivity to the desiccant inlet temperature and concentration and to the mass flow rate ratio. The inlet air temperature was set to 25 °C with a humidity ratio of 10 g/kg (relative humidity around 50%) with an air mass flux around 0.5 kg/m^{2}s. The packed column, 1 m in height, consists of 1″ plastic Pall Rings.

Firstly the influence of the inlet solution temperature was evaluated: Fig. 11 shows the humidity change through the column as a function of the inlet solution temperature under a desiccant mass flux of 1.0 kg/m^{2}s (mass flow rate ratio $L/G = 2$). The desiccant salt concentration (kg salt / kg solution) was set to 40% for LiCl solution, to 52% for LiBr and to 74% for KCOOH solution to have similar crystallisation temperatures (about −20 °C) and therefore a similar operating range. The solution inlet temperature shows a great influence on

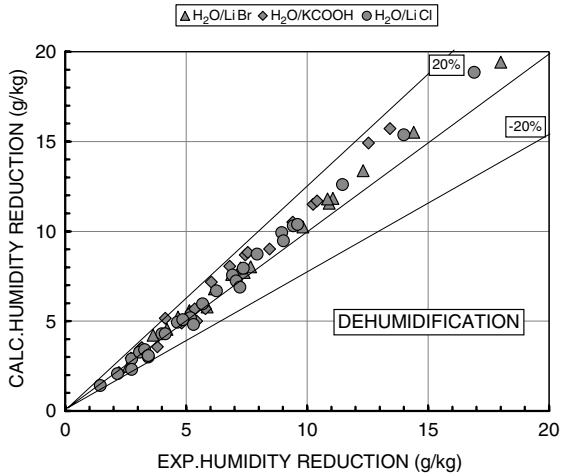

Fig. 8. Comparison between experimental and calculated dehumidification rates.

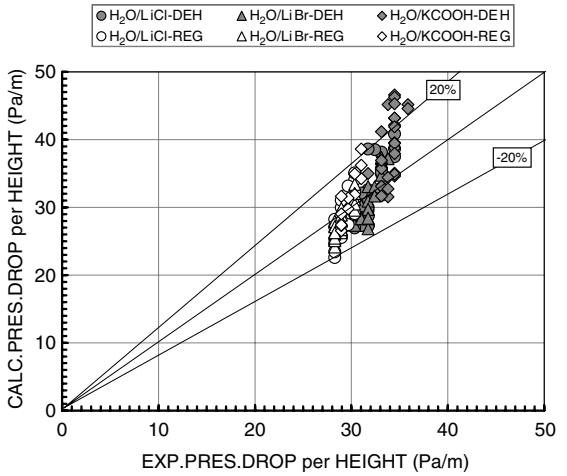

Fig. 10. Comparison between experimental and calculated pressure drop per unit height.

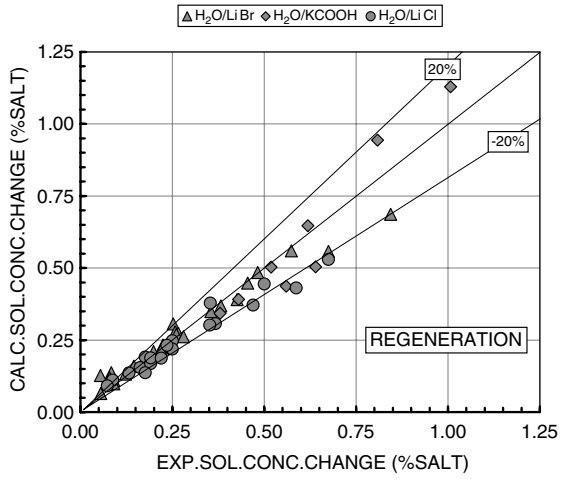

Fig. 9. Comparison between experimental and calculated regeneration rates.

the performance of the packed column: for each desiccant it is possible to determine a transition temperature which separates the dehumidification conditions (air humidity and desiccant salt concentration reduction) from the regeneration conditions (air humidity and desiccant salt concentration increase). For example, under the specific inlet operating conditions investigated in Fig. 11, H_2O/LiBr and H_2O/LiCl desiccants dehumidify the process air for an inlet solution temperature up to 40 °C, whereas for higher temperatures they are regenerated by the process air. The transition temperature for H_2O/KCOOH is around 37 °C. Consistent dehumidification rates are achievable in the temperature range from 20 to 30 °C, whereas regeneration process works well around 50 °C. Therefore it is possible to move from a dehumidification condition to a regeneration condition by simply increasing the solution inlet temperature by about 20–30 °C approximately.

Fig. 12 shows the humidity change through the column as a function of the inlet solution concentration under a solution mass flux at 1.0 kg/m^{2}s (mass flow rate ratio $L/G = 2$) and a solution inlet temperature at 25 °C. In this case for each desiccant it is possible to determine a transition concentration which separates

Table 4
Comparison between experimental data and simulation computer code

Test	Desiccant	Runs	Mean absolute deviation (dehumidification rate)	Mean absolute deviation (regeneration rate)	Mean absolute deviation (pressure drop)
Dehumidification	H_2O/LiCl	28	7.2%	=	9.2%
Dehumidification	H_2O/LiBr	20	7.7%	=	7.3%
Dehumidification	H_2O/KCOOH	26	11.4%	=	15.5%
Regeneration	H_2O/LiCl	19	=	13.2%	8.7%
Regeneration	H_2O/LiBr	26	=	17.3%	5.6%
Regeneration	H_2O/KCOOH	12	=	11.9%	8.9%

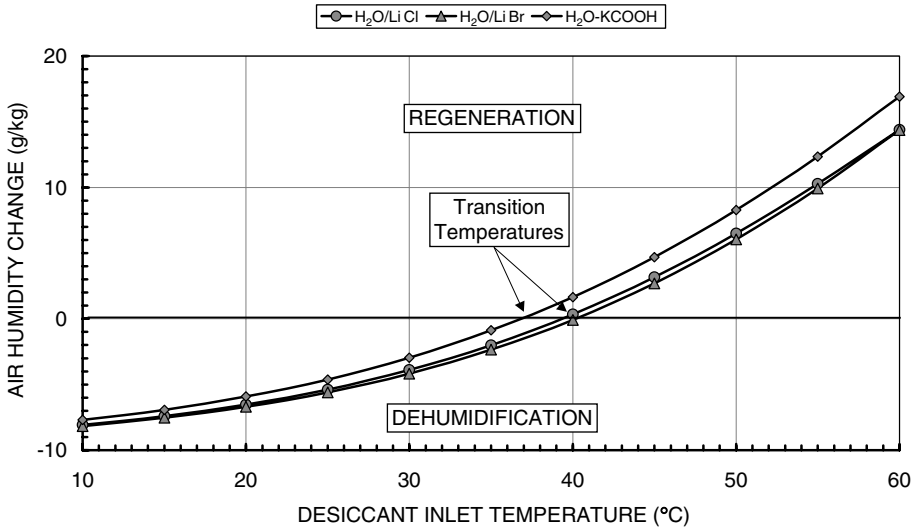

Fig. 11. Air humidity change vs. desiccant inlet temperature under packed column simulation.

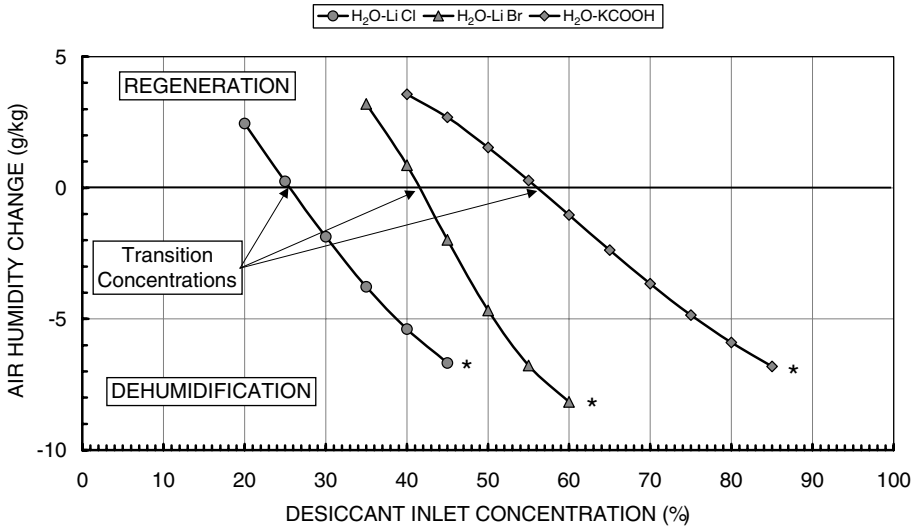

Fig. 12. Air humidity change vs. desiccant inlet concentration under packed column simulation.

the regeneration conditions from the dehumidification conditions. For example, under the specific inlet operating conditions investigated in Fig. 12, H_2O/LiCl shows the transition concentration between regeneration and dehumidification around 25% in salt, H_2O/LiBr around 42% in salt and H_2O/KCOOH around 57% in salt. An increase in solution concentration over the transition value produces an enhancement in the dehumidification rate up to the crystallisation conditions (* symbol in Fig. 12).

The influence of mass flow rate ratio L/G on air humidity change is shown in Fig. 13, where the humidity change is plotted vs. the ratio L/G. Fig. 13 refers to the following inlet operating conditions: LiCl concentration 40%, LiBr 52%, KCOOH 74%, solution inlet temperature at 25 °C for dehumidification and 50 °C for regeneration. The dehumidification and regeneration processes show a great sensitivity to this parameter for a flow rate ratio up to 2, whereas for higher ratios the sensitivity decreases quickly. Therefore it is possible to control the dehumidification and the regeneration rates in the packed column by changing the flow rate ratio L/G in the range from 0.5 to 2.

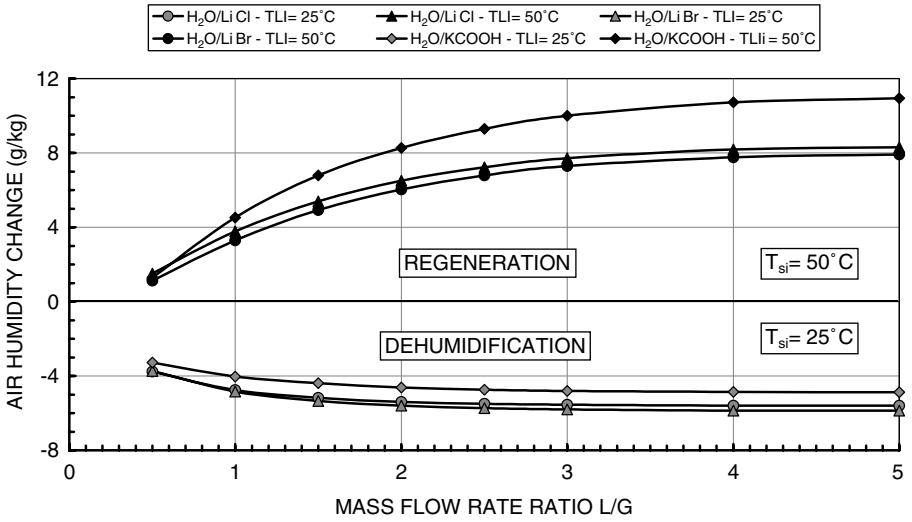

Fig. 13. Air humidity change vs. mass flow rate ratio under packed column simulation.

5. Conclusion

This paper presents the experimental tests and a simulation computer code of the sorption dehumidification of air by liquid desiccant and desiccant regeneration in a packed column: a fair agreement was found between experimental tests and simulation. Therefore the developed computer model can be considered a useful tool for predicting the performance of the system and analysing the system sensitivity to the main operating parameters.

The experimental tests and the simulations show that chemical dehumidification of air by liquid desiccant ensures consistent reduction in humidity ratio, which is suitable for applications to air conditioning or drying processes. Moreover, desiccant regeneration requires a temperature level around 40–50 °C which can be easily obtained by using solar energy or heat recovered from an industrial process or from a thermal engine.

The traditional solutions H_2O/LiCl and H_2O/LiBr present a better dehumidification performance than new solution H_2O/KCOOH which performs better in regeneration tests. However the new solution H_2O/KCOOH, less corrosive and expensive than traditional desiccants and fully compatible with the environment, allows humidity reductions of interest for technical applications.

References

[1] B. Kovac, P.R. Heimann, J. Hammel, The sanitizing effect of desiccant-based cooling, ASHRAE J. 39-I (1997) 60–64.
[2] Kathabar technical information, www.kathabar.com, 2001.
[3] DryKor technical information, www.drykor.com, 2001.
[4] R. Treybal, Mass Transfer Operations, McGraw Hill, New York, 1980, pp. 187–219, 314–322.
[5] H.M. Factor, G. Grossman, A packed bed dehumidifier/regenerator for solar air conditioning with liquid desiccants, Solar Energy 24 (1980) 541–550.
[6] P. Gandhidasan, M. Rifat Ullah, C.F. Kettelborough, Analysis of heat and mass transfer between a desiccant-air system in a packed tower, ASME J. Solar Energy Eng. 109 (1987) 89–93.
[7] D.I. Stevens, J.E. Braun, S.A. Klein, An effectiveness model of liquid-desiccant system heat/mass exchangers, Solar Energy 42 (1989) 449–455.
[8] A.Y. Khan, H.D. Ball, Development of a generalized model for performance evaluation of packed-type liquid sorbent dehumidifiers and regenerators, ASHRAE Trans. 98 (1992) 525–533.
[9] V. Martin, H.D. Ball, Effectiveness of heat and mass transfer processes in a packed bed liquid desiccant dehumidifier/regenerator, HVAC&R Res. 6 (2000) 21–39.
[10] P. Gandhidasan, A simplified model for air dehumidification with liquid desiccant, Solar Energy 76 (2004) 409–416.
[11] G.O.G. Löf, T.G. Lenz, S. Rao, S. Coefficients of heat and mass transfer in a packed bed suitable for solar regeneration of aqueous lithium chloride solution, ASME J. Solar Energy Eng. 106 (1984) 387–392.
[12] P. Patnaik, T.G. Lenz, G.O.G. Löf, Performances studies for an experimental solar open-cycle liquid desiccant air dehumidification system, Solar Energy 44 (1990) 123–135.
[13] A. Ertas, P. Gandhidasan, I. Kiris, E.E. Anderson, Experimental study on the performance of a regeneration tower for various climatic conditions, Solar Energy 53 (1994) 125–130.
[14] R.M. Lazzarin, A. Gasparella, G.A. Longo, Chemical dehumidification by liquid desiccant: theory and experiment, Int. J. Refrigeration 22 (1999) 334–347.

[15] N. Fumo, D.Y. Goswami, Study of an aqueous lithium chloride desiccant system: air dehumidification and desiccant regeneration, Solar Energy 72 (2002) 351–361.
[16] K. Gommed, G. Grossman, F. Ziegler, Experimental investigation of LiCl-water open absorption system for cooling and dehumidification, in: Proceedings of Int. Absorption Heat Pump Conf., Shanghai (P.R. China), September 24–27, 2002, 391–396.
[17] G.A. Longo, A. Gasparella, Experimental analysis on chemical dehumidification of air by liquid desiccant and desiccant regeneration in a packed tower, ASME J. Solar Energy Eng. 126 (2004) 587–591.
[18] V. Engel, J. Stichlmair, W. Geipel, A new correlation for pressure drop, flooding and holdup in packed columns, in: Proceedings of AICHE Annual Meeting, Miami, October, 1998.
[19] J. Stichlmair, J.L. Bravo, J.R. Fair, General model for prediction of pressure drop and capacity of countercurrent gas/liquid packed columns, Gas Sep. Purif 3 (1989) 19–28.
[20] E.F. Johnson, M.C. Molstad, Thermodynamic properties of aqueous lithium chloride solution, Final Report of Project H-1, University of Pennsylvania, 1949.
[21] Gmenlins Handbuch der Anorganischen Chemie, Das system LiCl–H_2O, Verlag Chemie, Weinheim (1960) 336–356.
[22] T. Uemura, Studies of the lithium chloride–water absorption machine, Technology report of the Kansai University, no. 9, 1967, pp. 71–88.
[23] L. McNeelly, Thermodynamic properties of aqueous solutions of lithium bromide, ASHRAE Trans. 85 (1979) 412–434.
[24] H. Loewer, Thermodynamische eigenschaften und warmediagramme des binaren systems lithiumbromid wasser, Kaltetechnik (1961) 178–184.
[25] H. Loewer, Dichte, spezifische warme, warmeleitzahl, dynamische viskosität der wasseringen lithiumbromid lösung, Kältetechnik (1961).
[26] H.M. Hellmann, G. Grossman, Improved property data correlations of absorption fluids for computer simulation of heat pump cycles, ASHRAE Trans. 102 (1) (1996) 980–996.
[27] S. Riffat, Private communications, 1998.
[28] S.J. Kline, F.A. McClintock, Describing uncertainties in single-sample experiments, Mech. Eng. 75 (1953) 3–8.